Pergamon

Int. J. Heat Mass Transfer. Vol. 38, No. 17, pp. 3285–3293, 1995

0017-9310/95 $9.50+0.00

0017-9310(95)00089-5

Measurement and interpretation of growth of monodispersed water droplets suspended in pure vapor

F. PETERS and K. A. J. MEYER
Universität Essen, Schützenbahn 70, 45127 Essen, Germany

(*Received* 21 *October* 1994)

Abstract—A piston expansion tube in combination with Mie light scattering is used to investigate growth of monodispersed water droplets due to condensation of surrounding pure vapor. The droplets are generated by homogeneous nucleation from the vapor phase and are observed in the size range 1.6–14×10^{-7} m which lies in the transition regime around Knudsen number 1. A model bridging between molecular and continuous heat and mass transfer processes is formulated on the basis of the well-known three-layer concept (droplet–collision-free zone–continuum). It includes a uniform pressure hypothesis which saves using the complicated energy equation in the collision-free zone. Consistent agreement with experimental results is found when only a minor adjustment factor is used.

1. INTRODUCTION

Dropwise condensation of vapor in a carrier gas is more frequently encountered in technical and natural situations than dropwise condensation of pure vapor. The most prominent pure vapor case occurs in the rapid expansion of a steam turbine in which homogeneous nucleation is induced followed by droplet growth. For the calculation of the steam flow as well as for the interaction of droplets with blades and walls, the growth rates are of great importance. Besides the application background the pure vapor case is an attractive one to study because it is not obscured by mass diffusion and other carrier gas effects. Such an elementary case is very useful in understanding condensation, particularly when it takes place, as in this work, around Knudsen number 1, where a transition model of mass and heat transfer becomes necessary.

The literature is not short of theoretical studies on droplet condensation (e.g. refs [1, 2]). The ultimate goal of theoretical work is to solve Boltzmann's transport equation for the non-equilibrium condensation and evaporation cases. Linearized equations assuming small deviations from equilibrium are mostly used for practical calculations. Experimental verification of existing theory is rather scarce. The pure vapor case has been treated in a very general way by Young [3], referring to essential references. For our present work we do not just use Young's equations because we were unable to apply them to our experiments satisfactorily. We formulate a working model simplified by: (i) a uniform pressure hypothesis which saves the treatment of the complicated energy equation in the molecular regime; (ii) a simple interpretation of the Schrage correction; and (iii) omitting the evaporation and condensation coefficients. From previous work [4] we think that these coefficients are either unity or at least very close to unity when the condensation surface is not contaminated, which is the case for droplets growing on homogeneous nuclei. Literature values vary widely and should always be seen in connection with the respective experimental conditions (compare Carey's [5] discussion).

Our model provides a set of equations suitable for comparison with our experiments. The model needs only a slight correction factor to fit the experimental data.

To our knowledge, no experimental work has been done on the pure vapor case in the transition regime. Our experimental approach is from the vapor/carrier system which we have studied extensively with a shock tube method [4]. There the gas dynamics of a shock tube is used to generate homogeneous nuclei serving as condensation sites in a supersaturated vapor/carrier atmosphere. Carrier gas experiments are easier to conduct due to the higher involved total pressures. Pure vapor experiments require a different device which we call the piston expansion tube (pex-tube). Most of the measuring techniques around this tube have been developed in connection with the shock tube experiments so that this work relies heavily on the previous one.

2. MODEL

Consider first phase equilibrium between liquid and vapor at a flat surface [Fig.1(a)]. Both bulk phases are at rest and have uniform temperature and pressure. The pressure, called the equilibrium vapor pressure over a flat surface, p_e, is a known function of T.

NOMENCLATURE

A	surface
c_p	isobaric specific heat capacity
d	diameter
h	enthalpy
k	thermal conductivity
k_B	Boltzmann constant
L	latent heat of condensation
$\dot{m}$	mass flux
p	pressure
$\dot{Q}$	heat flux
r	radius
R	specific gas constant
t	time
T	temperature
u	bulk velocity
v	molecular velocity.

Greek symbols

β	impingement rate
λ	mean free path
ρ	density
σ	surface tension.

Subscripts

d	droplet
e	equilibrium
i	interface
l	liquid
m	molecular
v	vapor.

Kinetic theory of gases predicts that vapor molecules hit the surface at the rate

$$\beta_e = \frac{p_e}{\sqrt{2\pi RT}} \tag{1}$$

which is written in the dimension of the mass flux density, i.e. number of molecules times molecular mass per unit area and time. As mentioned in the Introduction, we work with a condensation coefficient of unity from the beginning. Therefore, the molecules condense at the rate β_e. To maintain equilibrium the molecular fluxes to and from the surface must be equal, i.e. molecules escape from the liquid at the same rate as they condense.

Let the condensation exceed evaporation and keep the surface stationary [Fig. 1(b)], then the vapor of density ρ_v flows at the bulk velocity u_v towards the surface of area A where it condenses at the net rate $\dot{m} = -\rho_v u_v A$. (Note the sign convention: negative means condensation. All equations apply equally well to condensation or evaporation.) Continuity requires that the liquid proceeds to the left at a correspondingly much smaller velocity. Since net condensation indicates deviation from phase equilibrium, either the temperature or the pressure or both must deviate from equilibrium values. In principle temperature and pressure gradients may act as driving potentials.

Suppose the liquid conducts the heat of condensation very effectively, then the surface stays at T and thus also the vapor. The temperature is excluded as a driving potential and only the pressure of the bulk vapor differs from its equilibrium value. We use this idealization to contrast the droplet case below. The question now is how the net condensation rate depends on pressure. A bulk transfer equation involving pressure does not exist in this situation. The answer lies in molecular transfer. Evaporating molecules collide with vapor molecules about a mean free path away from the surface and vapor molecules coming from that distance reach the surface without collision. Accordingly the layer between the surface and interface to the bulk vapor is called a collision-free zone. We consider the mass flux across any fixed plane between the fixed surface and the fixed interface. The evaporation flux, being based on the unchanged liquid temperature, remains the same, i.e. $\beta_e A$. From the interface we have the impingement rate β_v and the flux $\beta_v A$; however, this is not the total mass flux because the vapor molecules are released from a base which itself moves at u_v causing the additional flux $\rho_v' u_v A$. Here ρ_v' is the density of the incoming vapor molecules in the collision-free zone. The net condensation flux then becomes

$$\dot{m} = \beta_e A - \beta_v A - \rho_v' u_v A \tag{2}$$

or after inserting the corresponding β and rearranging

$$\dot{m} = A \frac{\dfrac{p_e}{\sqrt{2\pi RT}} - \dfrac{p_v}{\sqrt{2\pi RT}}}{1 - \dfrac{\rho_v'}{\rho_v}}. \tag{3}$$

If we are not too far from equilibrium the densities of incoming and outgoing molecules are approximately equal, so that $\rho_v = 2\rho_v'$. Hence the net condensation rate is twice the rate obtained when only the impingement rates are considered, which is the case in the Hertz–Knudsen model. The factor 2 is associated with

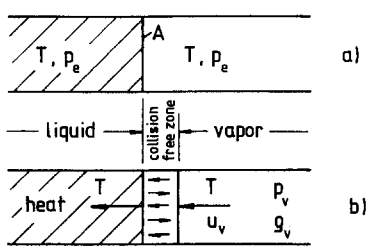

Fig. 1. Three layer concept used for condensation modelling at a plane surface.

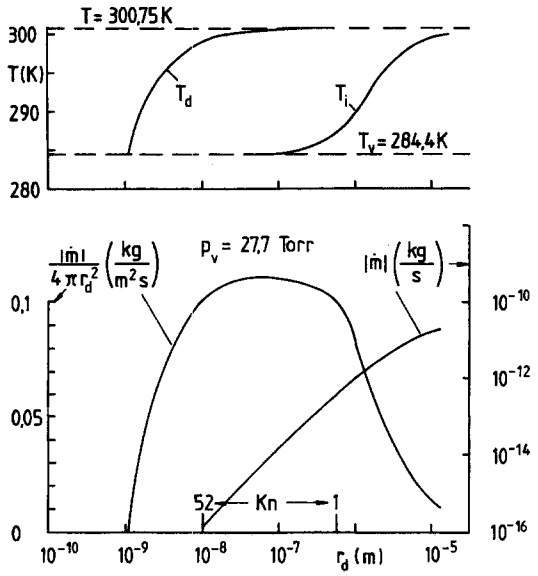

Fig. 2. Model calculations for water of droplet temperature T_d, interface temperature T_i, mass flux density $\dot{m}/4\pi r_d^2$ and mass flux $\dot{m}$ as a function of droplet radius r_d for a given vapor state (T_v, p_v).

Schrage [6]. In principle the factor is less than 2 depending on $\dot{m}$. Barrett and Clement [1] obtained 1.7.

In contrast to the plane surface case the droplet case exhibits two principal differences:

(i) The heat of condensation cannot be conducted away or transferred to a reservoir. The droplet has to give it off to the incoming vapor. A counterflow of heat and mass is established. Temperature will be a driving potential while pressure may be a driving potential.

(ii) The plane surface one-dimensional geometry is replaced by a spherical one described by the radius originating in the center of the droplet. The bulk vapor flow outside the collision-free zone is a spherical sink flow with acceleration and a corresponding pressure drop. Inside the collision-free zone the incoming molecules are not forced to proceed to the center. Not all of them hit the surface. Before evaluating the net condensation rate by molecular fluxes in analogy to the first case we need to deal with mass and heat transfer in the bulk vapor because the vapor state at the interface could differ from the ambient state which we locate (in principle) at infinity, $r \to \infty$.

To estimate the order of magnitude of the pressure drop between infinity and the interface we apply Bernoulli's law along a radial streamline using an average value for the density. Taking into account that $u \to 0$ as $r \to \infty$ we obtain for the pressure drop

$$\Delta p = \frac{1}{2\rho_v}\left(\frac{\dot{m}}{4\pi r_d^2}\frac{r_d^2}{r_i^2}\right)^2. \tag{4}$$

The purely computational maximum of Δp is found by inserting values of the greatest mass flux density $\dot{m}/4\pi r_d^2$ (see Fig. 2) and the smallest vapor density (0.01 kg m^{-3}) while letting r_d/r_i go to unity. It turns out that the pressure drop will not exceed 10^{-2} mbar which is small in comparison with even the lowest involved vapor pressure (20 torr). Hence, we are dealing with a negligible error by assuming uniform bulk pressure, which in particular means $p_i = p_v$.

The temperature distribution may be inferred from the energy equation which we write between infinity and the interface as

$$\dot{m}h_v + \dot{Q}_v = \dot{m}h_i + \dot{Q}_i. \tag{5}$$

We have already dropped the kinetic energy terms. At infinity the kinetic energy goes to zero and at the interface it turns out to be negligible in comparison with the enthalpy. $\dot{Q}_i$ is the heat flux entering the bulk vapor at the interface. It is equal to the latent heat of condensation

$$\dot{Q}_i = -\dot{m}L \tag{6}$$

with a negative sign because heat and mass are counterflowing. Division of equation (5) by equation (6) yields

$$\frac{c_p}{L}(T_v - T_i) = \frac{\dot{Q}_v - \dot{Q}_i}{\dot{Q}_i}. \tag{7}$$

With the ratio of $c_p/L \approx 0.8 \times 10^{-3}$ K^{-1} for water vapor the relative change of the heat flux (right side) would be below 1% at the highest expected temperature difference of 10 K. Accepting this error allows us to treat $\dot{Q}$ as a constant and to apply Fourier's law for a spherical system in the simplest form

$$\dot{Q} = -4\pi r^2 k\frac{dT}{dr} = \text{const.} \tag{8}$$

It provides a $1/r$ temperature distribution of the form

$$\frac{T - T_v}{T_i - T_v} = \frac{r_i}{r} \tag{9}$$

and a corresponding heat flux

$$\dot{Q} = 4\pi k r_i (T_i - T_v). \tag{10}$$

Using equation (6) again yields the temperature mass flux relationship

$$\dot{m} = -4\pi\frac{k}{L}r_i(T_i - T_v). \tag{11}$$

We now write down the mass flux in the collision-free zone surrounding the droplet. Molecules are leaving the interface at the rate β_i based on p_v and T_i. As mentioned before, not all of them hit the surface. The fraction which does and condenses is $\beta_i 4\pi r_d^2$. The others cross the collision-free zone and re-enter the interface. As discussed in the plane surface case, these molecules come from a base which itself moves at a velocity u_v producing the correction term $\rho_v' u_v 4\pi r_d^2$. The flux leaving the droplet is determined by the liquid temperature T_d which we take to be uniform throughout the droplet due to its smallness. This flux $\beta_e 4\pi r_d^2$

equals the one that would enter the droplet if the droplet was at phase equilibrium with the vapor at the same temperature. It thus depends on the equilibrium vapor pressure $p_e(T_d)$ which is a function of T_d. The resulting condensation mass flux is:

$$\dot{m} = \beta_e 4\pi r_d^2 - \rho_v' u_v 4\pi r_d^2 - \beta_i 4\pi r_d^2 \tag{12}$$

and after division by the bulk flux at the interface $\dot{m} = -\rho_v u_v 4\pi r_i^2$

$$\dot{m} = 4\pi r_d^2 \frac{\beta_e - \beta_i}{1 - \frac{\rho_v'}{\rho_v}\frac{r_d^2}{r_i^2}}. \tag{13}$$

Again, not too far from equilibrium the density ratio is approximately 1/2. After insertion of β we obtain

$$\dot{m} = 4\pi r_d^2 \frac{\frac{p_e(T_d)}{\sqrt{2\pi R T_d}} - \frac{p_i}{\sqrt{2\pi R T_i}}}{1 - \frac{1}{2}\frac{r_d^2}{r_i^2}}. \tag{14}$$

Taking T_v, p_v and the vapor properties as known quantities, there are two equations [equations (11) and (14)] for the three unknowns T_i, $\dot{m}$ and T_d. The additional equation would be the energy transfer equation for the collision-free zone which Young [3] obtained. Instead of that we use simple arguments concerning the pressure: (i) surface and interface pressures are equal; and (ii) the surface pressure is approximately equal to the phase equilibrium vapor pressure corresponding to the droplet temperature. We substantiate these arguments by interpreting the pressure as a momentum change of molecules as usual in gas kinetics.

The free molecular fluxes exchanged between surface and interface do not change momentum, entailing no pressure difference. Hence surface and interface pressures are equal. The surface pressure p_d is represented by the momentum change

$$p_d = \sqrt{(\pi/6)}[\beta_e v_d + (\beta_i + \rho' u_v) v_i] \tag{15}$$

or with equation (12)

$$p_d = 2\sqrt{(\pi/6)}\beta_e v_d \left(\frac{1}{2}\frac{v_i}{v_d} + \frac{1}{2}\right) - \sqrt{(\pi/6)}\frac{\dot{m}}{4\pi r_d^2} v_i \tag{16}$$

where v_i and v_d are mean velocities $\sqrt{3RT}$ of condensing and evaporating molecules, respectively. The factor of the bracket represents the equilibrium vapor pressure $p_e(T_d)$. We see that $p_d \to p_e$ as $v_i \to v_d$ while $\dot{m} \to 0$. Being smaller than unity the term in brackets reduces p_d with respect to p_e, accounting for the fact that the incoming molecules have less momentum than the leaving ones. The second term has the opposite effect (note $\dot{m} < 0$) reflecting that more mass enters than leaves the droplet. These counteracting influences keep the deviation of p_d from p_e very small. A few pars pro mille are estimated for the experimental conditions.

Regarding all this, T_d is simply calculated from the equilibrium vapor pressure. This has to take into account that the equilibrium vapor pressure over a curved surface is greater than that over a flat surface. Kelvin's equation provides the necessary correction in the form

$$p_e(T_d)_{curved} = p_e(T_d)_{flat} \exp\frac{2\sigma}{r_d \rho_l R T_d} \tag{17}$$

whereby p_{eflat} is the equilibrium vapor pressure [7]

$$p_e = \exp(21.125 - 2.7246 \cdot 10^{-2} T + 1.6853 \cdot 10^{-5} T^2 + 2.4576 \cdot \ln(T) - 6094.4642/T). \tag{18}$$

To sum up, we have obtained a set of equations [equations (11), (14) and (17)] to calculate T_i, T_d and $\dot{m}$ for the droplet case. The pressure plays a negligible role as a driving potential. This is due to the heat release from the droplet enforcing a temperature gradient ($T_d > T_i$) which at the same time acts as the driving potential for the mass transfer, as equation (14) makes clear. This is in contrast to the plane surface case where a temperature gradient is not enforced and the pressure drives the mass flux [equation (3)].

Some additional information is needed before equations (11), (14) and (17) can be solved. The mean free path is used in the form

$$\lambda = \frac{k_B T_i}{\sqrt{(2)}\pi d_m^2 p_v}. \tag{19}$$

The latent heat of condensation

$$L = 461.5[6094.4642 + 2.4576 T_d - 0.027246 T_d^2 + 3.3706 \cdot 10^{-5} T_d^2]\ [\mathrm{Nm\,kg^{-1}}] \tag{20}$$

is derived from Clausius–Clapeyron's equation, inserted into equation (18), while the heat conductivity k

$$k = [7.341 \cdot 10^{-3} - 1.013 \cdot 10^{-5} T + 1.801 \cdot 10^{-7} T^2 - 9.1 \cdot 10^{-11} T^3]\ [\mathrm{W\,m^{-1}\,K^{-1}}] \tag{21}$$

is taken from Reid *et al.* [8], and the surface tension from Pruppacher and Klett [9]

$$\sigma = 0.0761 - 1.55 \cdot 10^{-4}(T - 273.15). \tag{22}$$

Figure 2 shows a computed example illustrating the development of various quantities vs radius. The initial conditions are fixed by the vapor temperature $T_v = 284.4$ K and the vapor pressure $p_v = 27.7$ torr corresponding to the supersaturation of $S = 4.93$. We start with nuclei which are in metastable equilibrium with the vapor, i.e. their temperature is T_v and their size is predicted by Kelvin's equation [equation (17)],

$r_d = 1.11 \times 10^{-9}$ m. Growth starts with the addition of a single molecule. With the addition of mass latent heat has to be transferred causing T_d to rise with r_d. With growing radius the curvature influence is relaxed and T_d approaches the flat surface limit of 300.75 K.

The interface temperature T_i indicates best the transition between molecular and continuous transfer regimes which occurs around Knudsen number 1 ($Kn = \lambda/2r_d$). As long as the droplet is much smaller than the mean free path ($Kn \gg 1$) the transferred heat is too small to require noticable temperature difference $T_i - T_v$ in the bulk vapor. As $Kn \to 0$ an increasing $T_i - T_v$ is demanded. For big droplets the interface region practically disappears and T_i merges with the droplet temperature.

The temperature courses are apt to explain the culminating behavior of the mass flux density in the context of equation (14). With T_i constant and T_d rising the mass flux density obviously increases. Then T_d stagnates and T_i starts to grow, reversing the trend. The mass flux $\dot{m}$ itself may be approximated by a straight line in the double log scale. As a very crude estimate for the whole range $\dot{m}$ may be considered proportional to r_d^2. In connection with the law of mass conservation

$$\dot{m} = -\rho_l 4\pi r_d^2 \frac{dr_d}{dt} \tag{23}$$

the radius would then grow linearly in time.

3. EXPERIMENTAL METHOD

Homogeneous nucleation in the supersaturated state of a vapor is an excellent way of producing small growing droplets which are evenly distributed in space and monodispersed. We have shown this before [4] when studying droplets in carrier gases by means of a shock tube experiment. Unfortunately, the shock tube is not suitable for pure vapors because the pressures involved are too low for flawless operation of the diaphragm. To circumvent this problem we developed the pex-tube featuring a piston instead of the diaphragm. A full analysis of the pex-tube with its capabilities will be published elsewhere. Here, we restrict ourselves to a concise description.

The idea of the pex-tube is the following. An initially undersaturated vapor is subjected to a rapid expansion (a few milliseconds) ending at a supersaturated state. The degree of supersaturation corresponds to a certain nucleation rate [4] and a certain nuclear size given by the Kelvin equation [equation (17)]. Maintaining the supersaturated state for a short period, a defined number of nuclei come into existence. The nucleation period is short (e.g. 0.3 ms) because the rate is high (e.g. 10^7 cm^{-3} s^{-1}). The nuclei, practically born at an instant of time, grow into monodispersed droplets, the radius of which is measurable by Mie light scattering above 10^{-7} m.

Figure 3 shows how this is realized. The pex-tube is a closed system consisting of expansion and driver tube, buffer tank, filling bulb, vacuum pump and connecting lines. The system's vapor pressure is monitored by a baratron and all system parts are temperature controlled by electrical heating. The whole system is evacuated prior to filling with water vapor to a desired initial pressure. The vapor escapes from the liquid surface in the filling bulb when exposed to the evacuated system. The expansion tube (70 mm inner diameter) is confined by the observation window at one end and the expansion piston at the opposite end. Before the experiment it is separated from the rest of the system by valves. Displacement of the piston enlarges the expansion tube entailing pressure and temperature drop of the enclosed vapor. We have shown that the expansion is isentropic so that a single parameter determines the gas state. This parameter is the volume given by the piston displacement measured by an array of light barriers. The expansion pressure is measured simultaneously by a piezo transducer.

Vapor in front of the moving piston is discharged through a set of transfer ports into the exhaust chamber connected to the tank. Shortly before the piston comes to a stop it slides past another set of ports (recompression holes) releasing a small amount of vapor back into the expansion tube. This leads to a slight recompression following the end of the expansion. The nucleation period appears between the end of the expansion and the recompression. Besides the initial vapor pressure and temperature the state at nucleation is determined by the expansion ratio which is piston travel over tube length. Growth takes place at a slightly higher pressure and temperature after nucleation.

The expansion piston is attached to a rod which leaves the closed system through a pack of seals and extends into the driver tube. Here it carries two more pistons, the driver and the brake piston. The first runs in the driver tube (100 mm inner diameter) with a small clearance. When the driver tube is closed off against the atmosphere by a Mylar diaphragm and loaded with pressurized air (up to 5 bars) the clearance guarantees equal pressures on both sides of the piston. Breaking of the diaphragm causes a pressure drop across the piston resulting in a driving force and acceleration. The brake piston runs in its own tube with a built-in system of small damping ports (not shown) tuned to stop the three moving pistons exactly before the expansion piston hits the wall.

The growing droplets are observed by Mie light scattering. To this end an argon-ion laser passes the expansion tube close to the end wall window. Scattered light is received by a photomultiplier in the direction normal to the laser beam. The Mie signal identifies the droplet radius and by amplitude calibration yields the droplet number concentration at the same time. This system has been taken over from the previously mentioned shock tube experiment [4] and needs no further explanation at this point.

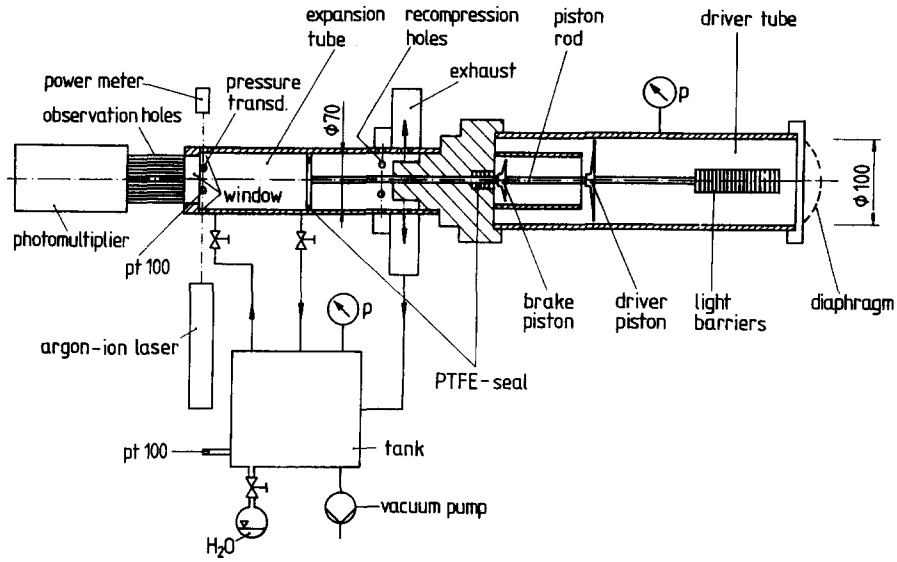

Fig. 3. Sketch of the piston expansion tube.

4. RESULTS AND COMPARISON WITH MODEL

4.1. *Measuring example*

Figure 4 gives a representative example of an experimental run providing traces of piston displacement, pressure and scattered light. The numbered steps of the piston displacement trace correspond to the light barriers, i.e. certain positions of the piston. From this information the expansion volume is inferred which converts into pressure and temperature of the nucleation period since we have an isentropic expansion. The pressure signal of the piezo transducer indicates the initial vapor pressure in the expansion tube (initial temperature T_1). After the piston is set into motion the pressure drops in an expansion of 7.4 ms followed by the nucleation period of 0.4 ms and a slightly elevated pressure. It turned out that due to the low pressure level the pressure transducer signal became rather noisy and useless for quantitative evaluation. This concerns the after-nucleation state of growth which cannot be derived from the piston displacement since the piston stops and mass is added through the recompression ports. However, the ratio of growth pressure to nucleation pressure is independent of total pressure, which means that the ratio can be taken from an experiment at higher total pressure (e.g. with air) which has a reliable pressure signal. For example, for the present experiments the growth pressure is found by multiplying the nucleation pressure by 1.032. The same factor applies to the temperature jump via the equation of state because the added mass is very small compared with the total mass.

The Mie scattering signal starts to rise straight after the nucleation period. In the course of time it exhibits peaks corresponding to certain radii of the scattering

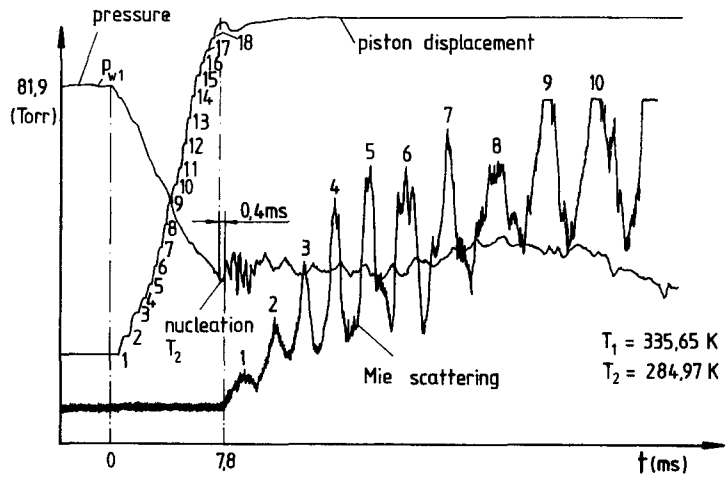

Fig. 4. Experimental run for water showing traces of pressure, piston displacement and scattered light.

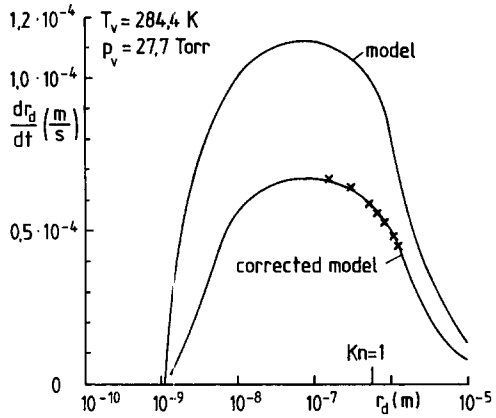

Fig. 5. Comparison of experimental (crosses) and theoretical growth rates for water droplets. Top curve: plain model. Bottom curve: model with adjustment factor.

droplets. The first peak identifies the radius 1.61×10^{-7} m. From calibration of the signal amplitude and the span of the nucleation period we conclude that in this experiment we have a nucleation rate of 4×10^6 cm^{-3} s^{-1} corresponding to 1.6 droplets growing in a volume of 1 mm^3. After approximately 30 ms the signal deteriorates. According to heat transfer calculations this is when the uniform temperature in the expansion tube begins to be heavily disturbed. Therefore heat transfer limits the observation time.

With each run it has to be checked whether vapor depletion or the release of latent heat affects the growth state. Calculations show that they have negligible influence for the present droplet sizes as long as less than 10 droplets are present in 1 mm^3 corresponding to a nucleation rate 10^7 cm^{-3} s^{-1}.

4.2. *Results*

Experimental results are on hand in terms of radius vs time plots ranging from 1.61×10^{-7} m (first peak) to 1.4×10^{-6} m. Each growth curve is fully determined by growth pressure p_v and temperature T_v.

A direct check of the model is best possible in terms of the growth rate which is the gradient of the radius vs time curve as shown in Fig. 5. The top curve represents the gradient of equation (23) after evaluation of $\dot{m}$ through the other equations. Note that the gradient is the same as the mass flux density of Fig. 2 divided by the liquid density. The crosses are from the experimental data. We see that the model overpredicts the experimental growth rates by a factor of about 1.6. Looking for an explanation we have checked the influence of the properties involved, the Schrage correction factor and the thickness of the collision-free zone which may not equal the mean free path. It turned out that the changes required to reconcile theory and experiment would be unreasonably large. The strongest influence comes from the difference of impingement rates in equation (14) in which the first term stands for evaporation and the second for condensation. Under our experimental conditions the difference is small compared with the rates themselves, therefore a relatively small error in one of the rates has a great effect on the difference, i.e. the mass flux. One possible error is the already addressed deviation of p_e from p_d concerning the first term. Another possible error is that the rate of the condensing molecules is in fact smaller than predicted. This can be accounted for by a condensation coefficient applied to the second term. In order to achieve agreement of the lower curve of Fig. 5 with experimental results we have either to increase the evaporation term by 1% or decrease the condensation term by 1%. Since the error cannot uniquely be attributed to condensation and since the correction is very small, a conclusion on the condensation coefficient other than that it is very close to one is not possible. It seems very important that the model correction is slight and consists only of a factor applying to all of our data.

The model representation of the $r(t)$ curves requires integration of equation (23). Integration starts straight after nucleation at the beginning of the growth period. The droplet radius at this point must be at least the Kelvin radius as given by equation (17), otherwise the droplet would decay and not grow. Figure 6 displays three experimental runs in comparison with the results of the integration. The agreement shows that the radius can be very well predicted as a function of time, although the integration covers two orders of magnitude of radius in the 'invisible' range before the first peak (dotted line). This may be considered as an indirect confirmation of the model in this range.

Figure 7 shows the influence of vapor depletion and heat release for a case in which the nucleation rate and thus the droplet number concentration is such that it counts. We see that growth is increasingly overpredicted when vapor depletion and heat release are ignored. Also the pure vapor case is compared with a vapor in air case (top, from previous work [4]) at the same vapor conditions and nucleation rate. Evidently air makes growth much faster. The reason is the heat transfer which is considerably enhanced by the air molecules which impinge, thermally accommodate and reflect. The enhanced heat transfer obviously dominates vapor diffusion through the carrier because diffusion retards mass transfer resulting in slower growth. This example indicates that one has to be careful with the often quoted statement that droplet condensation is diffusion controlled.

5. CONCLUSIONS

We have successfully applied a new experimental technique, the pex-tube, to measure growth of monodispersed water droplets carried in pure water vapor. Vapor state and droplet size were selected such that the measurements could be taken in the transition regime about Knudsen number 1.

An appropriate model has been derived including

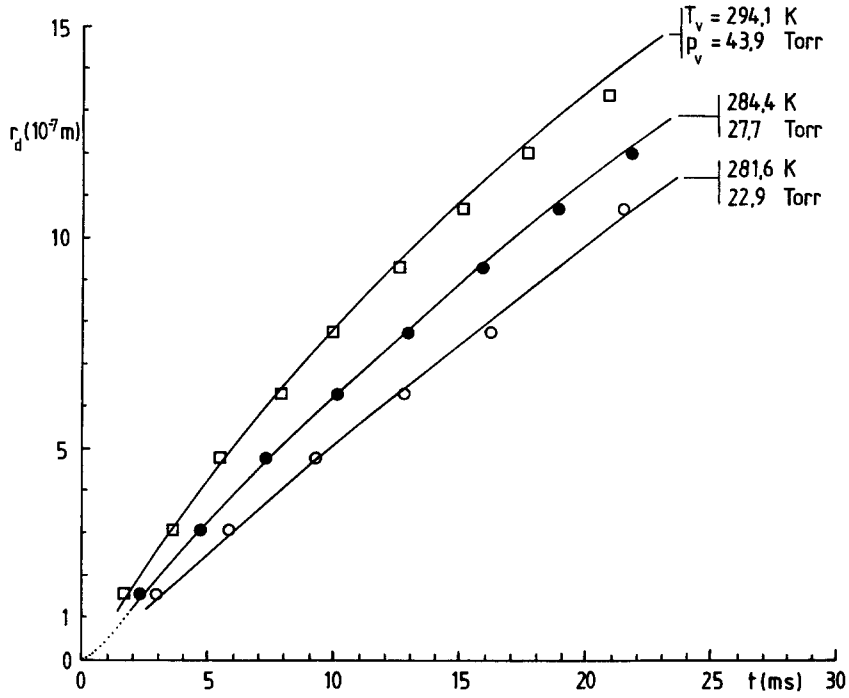

Fig. 6. Comparison of experimental (symbols) and theoretical growth of water droplets.

the classical Hertz–Knudsen expressions, a transition function with Schrage correction and a uniform pressure hypothesis. The latter means that ambient, interface and surface pressures are equal to the equilibrium vapor pressure corresponding to the droplet temperature. This allows the immediate determination of the droplet temperature from the ambient state saving the evaluation of the energy equation in the collision-free zone. The model is shown to agree with our experimental data over their entire range when a correction of 1% is applied either to the evaporation or to the condensation rate. In the first case the correction may be interpreted as a slight deviation from the pressure hypothesis. In the second case we could in principle refer to a condensation coefficient different from unity. However, the deviation is too small so that these experiments support what we have found before [4]: the condensation coefficient is either unity or very close to it when the condensation surface is clean, which seems to be the case for a droplet emanating from a homogeneous nucleus. The key feature of the present model is that it works with only a slight adjust-

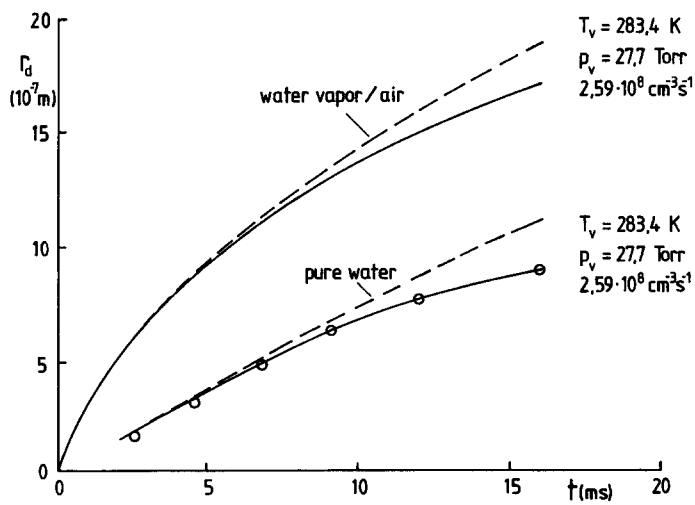

Fig. 7. Water droplet growth in pure vapor (lower curves) and in a vapor/air mixture (upper curves) at higher number concentrations (nucleation rate $> 10^8\ cm^{-3}\ s^{-1}$). Dashed curves: model predictions without vapor depletion and heat release. Solid curves: including both effects.

ment factor rather than a number of coefficients which cannot be determined independently.

Acknowledgement—This work was supported by grant Pe 401/3 of Deutsche Forschungsgemeinschaft (DGF).

REFERENCES

1. J. C. Barrett and C. F. Clement, Kinetic evaporation and condensation rates and their coefficients. *J. Colloid Interface Sci.* **150,** 352–364 (1992).
2. J. B. Young, The condensation and evaporation of liquid droplets at arbitrary Knudsen number in the presence of an inert gas. *Int. J. Heat Mass Transfer* **36,** 2941–2956 (1993).
3. J. B. Young, The condensation and evaporation of liquid droplets in a pure vapour at arbitrary Knudsen number, *Int. J. Heat Mass Transfer* **34,** 1649–1661 (1991).
4. F. Peters and B. Paikert, Measurement and interpretation of growth and evaporation of monodispersed droplets in a shock tube, *Int. J. Heat Mass Transfer* **37,** 293–302 (1994).
5. Van P. Carey, *Liquid–Vapor Phase-Change Phenomena.* Hemisphere, Washington (1992).
6. R. W. Schrage, *A Theoretical Study of Interphase Mass Transfer.* Columbia University Press, New York (1953).
7. D. Sonntag and D. Heinze, *Sättigunsdampfdruck und Sättigungsdampfdichtetafeln für Wasser und Eis.* VEB Verlag, Leipzig (1982).
8. R. C. Reid, J. M. Prausnitz and B. E. Poling, *The Properties of Gases and Liquids* (4th Edn). McGraw-Hill, New York (1987).
9. H. R. Pruppacher and J. D. Klett, *Microphysics of Clouds and Precipitation.* Reidel, Holland (1980).